Since January 2020 Elsevier has created a COVID-19 resource centre with free information in English and Mandarin on the novel coronavirus COVID-19. The COVID-19 resource centre is hosted on Elsevier Connect, the company's public news and information website.

Mathematical Biosciences 343 (2022) 108703

Contents lists available at ScienceDirect

Mathematical Biosciences

journal homepage: www.elsevier.com/locate/mbs

Original Research Article

Variant-specific interventions to slow down replacement and prevent outbreaks

Bushra Majeed, Marco Tosato, Jianhong Wu *

Laboratory for Industrial and Applied Mathematics, Department of Mathematics and Statistics, York University, Canada

ARTICLE INFO

Keywords:
COVID-19
Limited resources
Variant of concerns
Whole genome sequencing
Strain-specific interventions
Tracing delay

ABSTRACT

Emergency and establishment of variants of concern (VOC) impose significant challenges for the COVID-19 pandemic control specially when a large portion of the population has not been fully vaccinated. Here we develop a mathematical model and utilize this model to examine the impact of non pharmaceutical interventions, including the COVID-test (PCR, antigen and antibody test) and whole genome sequencing (WGS) test capacity and contact tracing and quarantine strength, on the VOC-induced epidemic wave. We point out the undesirable and unexpected effect of lukewarm tracing and quarantine that can potentially increase the VOC-cases at the outbreak peak time, and we demonstrate the significance of strain-specific interventions to either prevent a VOC-induced outbreak, or to mitigate the epidemic wave when this outbreak is unavoidable.

1. Introduction

Genetic mutations play an important role in the evolution of virus in general, and in the ongoing evolution and emergence of novel Severe Acute Respiratory Syndrome Coronavirus 2 (SARS-CoV-2) variants in particular [1]. These genetic variations can lead to emergence of new variants with selection of phenotypes increasing viral fitness (replication, transmissibility, immune escape).

Characterizations of these variants depend on the type and number of mutations [2,3]. For SARS-CoV-2, a "variant of interest" (VOI) can elevate to "variant of concern" (VOC), under the definition of the World Health Organization (WHO), when it transmits more quickly in a population than its ancestral lineage, and/or when it has the ability to evade natural or vaccine-induced immunity making available vaccines ineffective. Several variants of concern have indeed led to a large increase of incidence, hospitalization and mortality in many countries after more than a year of initial report of the COVID-19 outbreak. As of May 16, 2021, most common VOC internationally identified include: B.1.1.7 (identified in September, 2020) [4], B.1.351 (identified in October, 2020), P1 (identified in December, 2020) and B.1.617 (identified in December, 2020) [5–8]. Strain-specific interventions are needed in an already strained public health system where there is little additional resource available for mitigating VOC emergency and establishment.

Genome sequencing methods are used to decode the genes to better understand the virus mutations. Genomic sequencing permits recognition of pathogen, monitoring its evolution over time, and detecting appearance of a new variant [9]. Any VOC-specific intervention relies on the use of whole genome sequencing test to specify the strain. Here, we develop a modeling framework and analysis, in order to quantify the role of variant-specific interventions in preventing replacement and outbreak of the VOC under consideration. Obviously, this design and implementation of variant-specific interventions needs rapid whole genome sequencing (WGS) of confirmed cases, this in turn requires that (1) the total confirmed cases (for both the original or resident lineage and its variant) to be sufficiently small such that the time delay from contact tracing to testing and to case and strain confirmation can be minimized, and (2) the WGS can be performed on majority, if not all, COVID-19 test positive cases.

Some countries, such as South Korea, Australia and New Zealand have indeed used rapid testing, contact tracing, isolation and mandatory quarantining of international travelers as effective tools to keep case counts significantly low. The role of rapid tests to enhance contact tracing and quarantine/isolation for controlling past outbreaks has been modeled and analyzed [10–15], and other modeling studies have addressed VOC-relevant issues including evaluating the impact of increasing transmissibility and estimating the replacement time [5–8,16–19]. In contrast, we seek to evaluate, under different scenarios of clinical COVID-19 and WGS testing capacity, the impact of the co-circulation of old-lineage and VOC on testing delays, the impact of these delays on contact tracing and quarantine/isolation, and the impact of strain-specific contact tracing and quarantine/isolation measures on the disease spread potential and disease burden. In particular, we seek to answer the question of whether VOC-specific public health investments

* Corresponding author.
E-mail address: wujh@yorku.ca (J. Wu).

https://doi.org/10.1016/j.mbs.2021.108703
Received 18 June 2021; Received in revised form 8 September 2021; Accepted 8 September 2021
Available online 20 September 2021

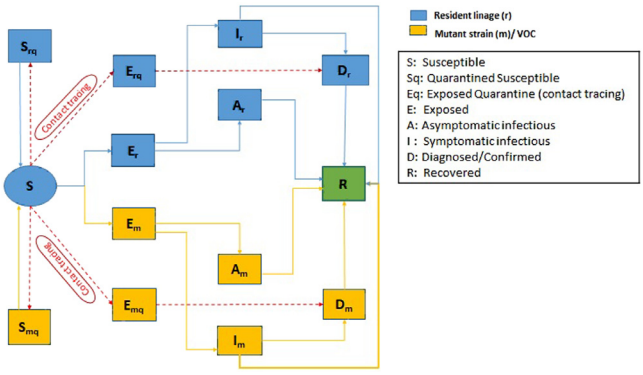

Fig. 1. The flowchart illustrating the COVID-19 infection dynamics with two strains, original resident strain (r-lineage) and mutant strain (m-variant)/VOC. Interventions including intensive contact tracing followed by quarantine and isolation are indicated.

and interventions can optimize the resources to avoid a new VOC-induced outbreak or, if this outbreak is unavoidable, to mitigate the outbreak.

2. Material and methods

2.1. Model formulation

We consider a scenario during a viral disease pandemic such as the COVID-19 global pandemic, when a combination of public health interventions, including social distancing, testing, quarantine and isolation, is used to mitigate an outbreak with some success while a variant of concern is introduced.

According to the World Health Organization (WHO) guidelines for referring to viral variants of SARS-CoV-2, a variant of interest (VOI) contains mutations thought to alter the phenotypic properties of the virus, with documented community transmission or international spread, and a variant of interest becomes a variant of concern (VOC) if the variant has increased transmission and virulence. We have in particular the SARS-CoV-2 and its variant B1.1.7 as a background pair though our setting and analysis apply to SARS-CoV-2 and other VOCs, including B.1.351, P1 and B.1.617.

In our model formulation, we use sub-index r for the original (resident) lineage, and m for the variant of concern being considered. For sake of simplicity, we assume both r-lineage and m-variant provide complete immunity to the other immediately on infection that will last for the entire period of the outbreak and so no co-infection can happen. Therefore, by a susceptible individual, we mean an individual that who is susceptible to both r-lineage and m-variant, and an individual recovered from infection with one of r-lineage and m-variant is completely immune to both. So, recovered will not return to susceptible class.

In our formulation, we stratify the population into 14 mutually exclusive compartments (Fig. 1) based on the epidemiological status of the individuals and the control interventions: susceptible (S), exposed with the r-lineage and its variant ($i = r, m$), (E_i), asymptomatic infectious (A_i), infectious with symptoms (I_i), diagnosed and isolated (D_i), isolated susceptible (S_{qi}), isolated exposed under contact tracing (E_{qi}) and recovered (R). Following the basic model structure developed by the LIAM group [20], we also consider contact tracing, where a proportion, q, of individuals exposed to the virus are traced and isolated. The quarantined individuals can either move to the compartment E_{qi} or S_{qi}, depending on whether the transmission has occurred (with probability β_i if the contact is with someone that has strain i), while the other proportion, $1-q$, consists of individuals exposed to the virus who are escaped from contact tracing and, therefore, move to the exposed compartment E_i once infected, or stay in the compartment S otherwise.

We assume that resident lineage and m-variant have different transmission probabilities and the VOC is more transmissible, i.e. $\beta_m > \beta_r$ with $\beta_m = \kappa\beta_r$, hence $\kappa > 1$.

Unlike the early model formulation, here we assume the testing (both COVID-19 testing to confirm cases and WGS testing for VOC) capacity is limited, and the quarantine proportion of traced contacts of cases confirmed by the testing is negatively proportional to the total number of individuals being tested. We describe this by the classical Holling-type II saturated function. In particular, let B be the total number of people needed to be tested. These include exposed individuals who have been traced, and those who are symptomatically infected (and have escaped from contact tracing when they were in their incubation period). That is,

$$B = E_{rq} + E_{mq} + I_r + I_m.$$

In what follows, we also write $I = I_r + I_m$ and $E_q = E_{rq} + E_{mq}$ Let w be the constant such that $1/w$ is the maximum number of people who can be tested per day(testing capacity per day). Let

$$H(B) = \frac{1}{1 + wB}.$$

Then H is a decreasing function, with $H(0) = 1$ and $H(\infty) = 0$. We use δ_I and δ_q to denote the fastest rate to diagnostically confirm a symptomatically infectious and a traced exposed individual, respectively. Then the practical rate to diagnostically confirm a symptomatically infectious and a traced exposed individual, is respectively given by $\delta_I H(B)$ and $\delta_q H(B)$, and the larger the B, the smaller the diagnostic confirmation rate. Therefore, the total number of individuals to be practically tested per day is given by the Holling-type II like function $(\delta_I I + \delta_q E_q)H(B)$. This, like the normal predator–prey model, assumes that processing of testing and searching for candidates to be tested are mutually exclusive behaviors. In this analogue, w is also the test processing time per individual. We mention that this formulation is similar to that in the Monod equation for the growth of microorganisms and that in the Michaelis–Menten equation for the rate of enzymatic reactions.

In what follows, we let

$$F_1(I, E_q) = \frac{\delta_I I}{1 + w(I + E_q)}$$

$$F_2(I, E_q) = \frac{\delta_q E_q}{1 + w(I + E_q)}$$

or, in terms of E_{rq}, E_{mq}, I_r, and I_q, separately, we have

$$F_{rI}(I_r, I_m, E_{rq}, E_{mq}) = \frac{\delta_{Ir} I_r}{1 + w(I_r + I_m + E_{rq} + E_{mq})}$$

$$F_{mI}(I_r, I_m, E_{rq}, E_{mq}) = \frac{\delta_{Im} I_m}{1 + w(I_r + I_m + E_{rq} + E_{mq})}$$

$$F_{rE}(I_r, I_m, E_{rq}, E_{mq}) = \frac{\delta_{rq} E_{rq}}{1 + w(I_r + I_m + E_{rq} + E_{mq})}$$

$$F_{mE}(I_r, I_m, E_{rq}, E_{mq}) = \frac{\delta_{mq} E_{mq}}{1 + w(I_r + I_m + E_{rq} + E_{mq})}$$

These functions characterize the saturation phenomenon of limited testing resources. All of the above saturated functions are C^1-smooth, and each reaches its peak or maximum at ∞, that is,

$$\lim_{I_i \to \infty} F_{iI} = \frac{\delta_{Ii}}{w}$$

and

$$\lim_{E_{iq} \to \infty} F_{iE} = \frac{\delta_{iq}}{w}$$

Since tracing happens as a consequence of testing with some delay, we can define the quarantine fraction q_r and q_m for both r-lineage and m-variant respectively as

$$q_r = q_{r0}(\tau_1)H(B(t - \tau_1)), \tag{1}$$

$$q_m = q_r + (1 - q_r)q_{m0}(\tau_2)H(B(t - \tau_2)). \tag{2}$$

In this formulation, we have

$$q_{r0}(\tau_1) = \begin{cases} q_{r0}\left(\frac{L-\tau_1}{L}\right), & \text{if } \tau_1 < L, \\ 0 & \text{otherwise,} \end{cases}$$

and similarly,

$$q_{m0}(\tau_2) = \begin{cases} q_{m0}\left(\frac{L-\tau_2}{L}\right), & \text{if } \tau_2 < L, \\ 0 & \text{otherwise.} \end{cases}$$

Here L represents the incubation period, and τ_1 and τ_2 are testing delays in clinical COVID-19 test and WGS test respectively. This formulation reflects the fact that the quarantine proportion decreases linearly as a function of the testing delay, and quarantine proportion becomes zero when the testing delay exceeds the incubation period. Here q_{r0} and q_{m0} represent the maximum quarantine fractions of confirmed COVID-19 tests and of mutants/VOC after WGS tests respectively. Because of similar symptoms, simple COVID-19 clinical diagnostic test can only confirm the infection but cannot identify m-variant from r-lineage. So, the contacts traced for both strains would be quarantined at the same rate, that is why q_r is added in Eq. (2). In addition, in Eq. (2), we model the quarantine rate of mutant strain if additional WGS test confirms the m-variant and extra efforts to trace and quarantine those exposed to the m-variant.

The constant delay τ_1 in Eq. (1) represents the time lag between COVID-19 confirmation of an index case and successful tracing and quarantine/isolation of its exposed contacts. Since WGS test is required to identify VOC type and this test often requires sending samples to a central lab for sequencing, there will be additional time lag between the WGS identification and this delay is denoted by $\tau_2 - \tau_1$. Therefore, any additional intervention to enhance the contact tracing and quarantine of m-variant will be implemented with the delay $\tau_2 = \tau_1 + (\tau_2 - \tau_1)$, hence the delay τ_2 in the second term of Eq. (2).

In practice, the capacity for WGS only allows for WGS testing for a small portion of COVID-19 diagnosed cases. Assuming these are randomly drawn, then the quarantine rate for m-variant cases must be modified as

$$q_m = q_r + (1 - q_r)q_{m0}(\tau_2)H_g(B(t - \tau_2)) \tag{3}$$

with

$$H_g = \frac{1}{1 + w_g B}$$

Here, $1/w_g = p(1/w)$ is the maximum WGS testing capacity per day, p is the proportion of clinically COVID-19 confirmed cases further tested for genetic sequence, and B is the total number of infected to be tested.

Under all these assumptions and incorporating saturated diagnostic functions, we end up with the following dynamical system of nonlinear equations:

$$S' = \sum_{i=r,m}\left[-(\beta_i c + cq_i(1 - \beta_i))S\frac{(I_i + \theta A_i)}{N} + \lambda S_{iq}\right] \tag{4}$$

$$E_i' = \beta_i c(1 - q_i)S\frac{(I_i + \theta A_i)}{N} - \sigma E_i \tag{5}$$

$$E_{iq}' = \beta_i cq_i S\frac{(I_i + \theta A_i)}{N} - F_{iE}(I_r, I_m, E_{rq}, E_{mq}) \tag{6}$$

$$S_{iq}' = (1 - \beta_i)cq_i(S)\frac{(I_i + \theta A_i)}{N} - \lambda S_{iq} \tag{7}$$

$$A_i' = \sigma(1 - \rho)E_i - \gamma_A A_i \tag{8}$$

$$I_i' = \sigma\rho E_i - F_{iI}(I_r, I_m, E_{rq}, E_{mq}) - (\alpha + \gamma_I)I_i \tag{9}$$

$$D_i' = F_{iI}(I_r, I_m, E_{rq}, E_{mq}) + F_{iE}(I_r, I_m, E_{rq}, E_{mq}) - (\alpha + \gamma_D)D_i \tag{10}$$

$$R' = \sum_{i=r,m}(\gamma_I I_i + \gamma_A A_i + \gamma_D D_i) \tag{11}$$

2.2. Basic reproduction number

In this section, we look at the basic reproduction number R_0, a centerpiece parameter in infectious disease dynamics (the average number of new infections per infected individual during its infectious period in a 'naive' population without any public health interventions). Typically, if the value of the reproduction number is greater than 1, disease would persist in a population and continue to spread, and if it is less than 1, the epidemics would decline gradually and eventually die out.

The basic reproduction number of this two strain transmission model with control interventions such as contact tracing and isolation, the R_{c0} control/effective reproduction number, is given by

$$R_{c0} = \max(R_{r0}, R_{m0}).$$

Using the standard next generation matrix approach [21,22] applied to the case when delays, τ_1, τ_2 equal to zero. in Eqs. (1) and (2), we get the following control reproduction number for both r-lineage and m-variant respectively as

$$R_{r0} = \frac{\beta_r c\rho(1 - q_{r0})}{\delta_I + \alpha + \gamma_I} + \frac{\beta_r c\theta(1 - \rho)(1 - q_{r0})}{\gamma_A}, \tag{12}$$

and

$$R_{m0} = \frac{\beta_m \rho c(1 - q_{r0})(1 - q_{m0})}{\delta_I + \alpha + \gamma_I} + \frac{\beta_m c\theta(1 - \rho)(1 - q_{r0})(1 - q_{m0})}{\gamma_A}. \tag{13}$$

In particular, R_{m0} can be written in terms of R_{r0} as

$$R_{m0} = \kappa(1 - q_{m0})R_{r0}, \tag{14}$$

where $\kappa = \frac{\beta_m}{\beta_r}$, $(\kappa > 1)$ is the ratio of the transmission probability (the relative infectivity) of m-strain over the r-lineage. In Eq. (14), $1 - q_{m0}$ represents the effect of a contact tracing strategy targeted to VOC to reduce the number of secondary infections of mutant strain in the community/population.

Lemma 2.2.1. *The following results hold for R_{r0} and R_{m0}:*

(i) $R_{r0} = R_{m0} \iff q_{m0} = 1 - \frac{1}{\kappa}$;
(ii) If $R_{r0} < \frac{1}{\kappa}$, *then* $R_{m0} < 1$;
(iii) If $R_{r0} \geq \frac{1}{\kappa}$, *then* $R_{m0} < 1 \iff q_{m0} > 1 - \frac{1}{\kappa R_{r0}}$.

Proof. Using Eq. (14) to replace R_{m0} in $R_{r0} = R_{m0}$, it derives that $q_{m0} = 1 - \frac{1}{\kappa}$. Let $R_{r0} > \frac{1}{k}$, we analyze when $R_{m0} < 1$. Using Eq. (14), we have

$$\kappa(1 - q_{m0})R_{r0} < 1.$$

By isolating q_{m0}, we get

$$q_{m0} > 1 - \frac{1}{\kappa R_{r0}}. \tag{15}$$

Note that $0 \leq q_{m0} \leq 1$, since it is a fraction. If $R_{r0} < \frac{1}{k}$, (15) always holds therefore $R_{m0} < 1$. If $R_{r0} \geq \frac{1}{k}$, then (15) has to hold in order for $R_{m0} < 1$.

Further Eq. (14) with $\kappa > 1$ and $q_{m0} \in [0, 1]$ implies that there are four generic possibilities.
(I) $R_{r0} < 1$

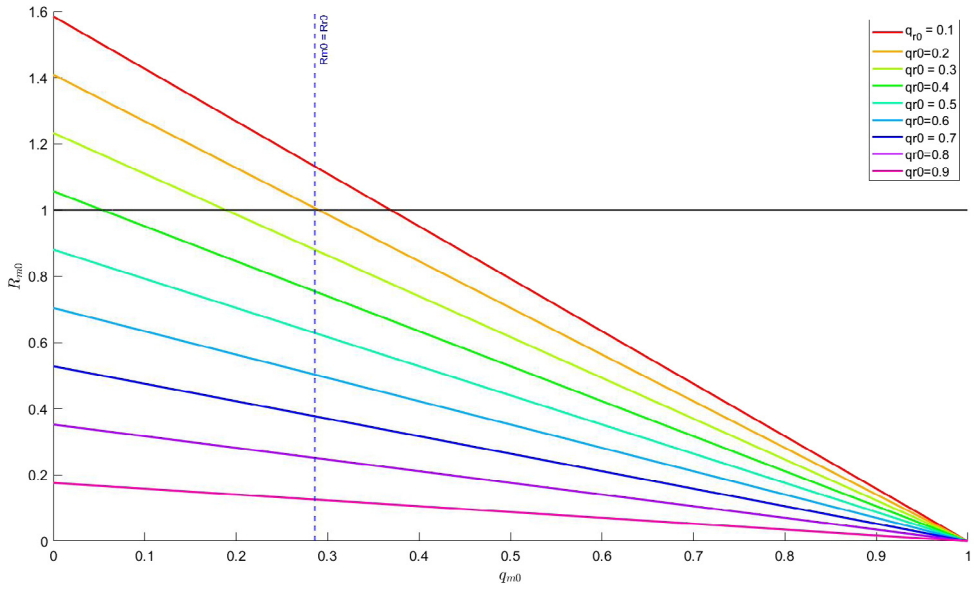

Fig. 2. Plot of R_{m0} as a function of q_{m0}. There is a linear relationship between reproduction number R_{m0} and strain-specific quarantine fraction q_{m0} when q_{r0} is fixed. Here the vertical dotted line represents the value of $q_{m0} \approx 0.2857$ at which $R_{m0} = R_{r0}$ and horizontal line represents threshold value of $R_{m0} = 1$.

(a) $R_{m0} < 1$ for all quarantine choices if $R_{r0} < 1/\kappa$ (i.e. if basic reproduction number for resident strain is very small) guarantees that both strains die out.
(b) $R_{m0} > 1$ if $R_{r0} > 1/\kappa$ and $q_{m0} < 1 - \frac{1}{\kappa R_{r0}}$ (i.e. if quarantine rate is too small and basic reproduction number for resident strain is larger than the threshold $\frac{1}{\kappa}$) would lead to persistence of a mutant strain and extinction of the resident strain.
(II) $R_{r0} > 1$
(c) $R_{m0} < 1$ if $q_{m0} > 1 - \frac{1}{\kappa R_{r0}}$ (i.e. if quarantine rate for mutant strain is large enough) would lead to the resident strain becoming prevalent.
(d) $R_{m0} > 1$ if $q_{m0} < 1 - \frac{1}{\kappa R_{r0}}$ (i.e. if quarantine rate for mutant strain is smaller than a threshold) would guarantee coexistence of the strains.

2.3. Parameters

We have used some data from the Province of Ontario, Canada as a case study for our model simulations. We start with the assumption that resident lineage is under control, i.e. its reproduction number is less than 1. We fix the following parameters: the probability of transmission of resident lineage $\beta_r = 0.1446$, contact rate $c = 5.78$ and the fastest diagnostic rate $\delta_I = 0.333$, such that the value of R_{r0} stays less than 1, for any quarantine rate q_r less than 0.3. We assume that these parameter values do not change over the simulations we conduct with the introduction of the VOC. We consider the incubation period as 5 days (mean 5–6 days, range 1–14 days) [23] for both resident and VOC. Even though relative transmissibility of VOCs ranges from 140% to 160% [16,17], we use the conservative assumption that $\beta_m = 1.4\beta_r$, which represents a 40% increase in transmission of m-strain compared to resident lineage. All other parameters are taken from [20], given in Table 2 and we assume that the relevant parameters, except the transmission probability per contact, are the same for the r-lineage and m-strain. We note that it takes usually 2–3 days from sampling to the return of results, so, our assumed fastest diagnose rate of symptomatic infected individuals seems plausible.

We consider the initial values of model variables for r-lineage as estimated in [20] according to the data from the end of December 2020. We assume that when the first few cases of mutant strain were diagnosed in Ontario, resident lineage was predominant and the initial frequency of the VOC was very low (about 0.1%) relative to the r-lineage. So, initial values for m-strain variables are chosen accordingly given in Table 1. Furthermore, we assume that the resources allow for a maximum 40%–70% of tracing coverage (proportion of contacts that are successfully traced and isolated) after the clinical COVID-19 test (see Table 1).

2.4. When and how VOC-specific intervention is needed?

In this subsection, we conduct some numerical experiments to see when and how VOC-specific interventions such as additional quarantine and rapid WGS testing are needed.

2.4.1. Reproduction number: full control

The control reproduction number of the VOC with higher transmissibility plays a dominating role to determine whether a VOC-induced outbreak can be prevented with the interventions, primarily contact tracking and quarantine/isolation.

Note that if the control reproduction number of the r-lineage $R_{r0} \geq 1$ or slightly below one, then R_{m0} will surely exceed the unity, so our focus is on conditions for the quarantine fractions of r-lineage and m-variant such that $R_{m0} < 1$.

Fig. 2 shows the linear relationship between R_{m0} and q_{m0} when q_{r0} is fixed, where each colored straight line corresponds to a fixed quarantine fraction for the traced exposed individuals. In this case, there is a threshold value of q_{m0} at which $R_{m0} = R_{r0}$, and this is given by the dotted vertical line. We use the horizontal line to represent the threshold $R_{m0} = 1$ so the intersection of the colored line with the horizontal line gives the minimal additional quarantine fraction for the exposed to the VOC in order to avoid the VOC-induced outbreak. For example, with a $q_{r0} = 0.3$ quarantine fraction for all exposed traced, we need an additional $q_{m0} = 0.2$ quarantine fraction of all those exposed to VOC in order to avoid an outbreak; however increasing $q_{r0} = 0.4$ will reduce the need of q_{m0} to about 0.05.

Fig. 3 gives isoclines of the control reproduction number R_{m0} as R_{r0} and q_{m0} vary. In particular, if R_{r0} is kept less than $\frac{1}{\kappa} \approx 0.7142$ (under our parameter assumptions), variant-specific contact tracing and additional quarantine would not be necessary. In other words, to control the epidemic and to slow disease progression without any strain-specific interventions, a goal is to ensure that $R_{r0} \leq \frac{1}{\kappa}$. In case this cannot be achieved, intensive contact tracing of VOC cases after WGS testing will be required, following the theoretical result in Lemma 2.2.1.

Table 1
Model variables and their initial values.

Variable List			
Variable	Definition	Initial Value	Source
S	Number of individuals susceptible to both strains	1.42033×10^7	Data
S_{rq}	Quarantined susceptible population with resident lineage	0.01617×10^7	[20]
S_{mq}	Quarantined susceptible population with mutant strain	0	chosen
E_{rq}	Quarantined exposed population with resident lineage	0.00123322×10^7	[20]
E_{mq}	Quarantined exposed population with mutant strain	2	chosen
E_r	Exposed population with resident lineage.	0.001177×10^7	[20]
E_m	Exposed population with mutant strain	10	chosen
A_r	Asymptomatic infectious with resident lineage	0.0004497×10^7	[20]
A_m	Asymptomatic infectious with mutant strain	0	chosen
I_r	Symptomatic infectious with resident lineage	0.000543029×10^7	[20]
I_m	Symptomatic infectious with mutant strain	5	chosen
D_r	Diagnosed isolated with resident lineage	0.0010226×10^7	[20]
D_m	Diagnosed isolated with mutant strain	2	chosen
R	Recovered from both strains	0.02905217×10^7	[20]

Table 2
Parameters, definitions and values.

Parameter List			
Parameter	Definition	Value	Source
β_r	Probability of transmission of resident lineage	0.1446	chosen
β_m	Probability of transmission of mutant strain	$1.4\times\ \beta_r$	chosen [16,17]
c	Contact rate	5.78	chosen
σ	Transition rate of exposed individuals to infected class	1/5	[23]
λ	Rate at which quarantine uninfected released to community	1/14	[20,24]
ρ	Probability of having symptoms from exposed class	0.724	[20]
α	Disease-induced death rate	0.008	[20]
γ_I	Recovery rate of symptomatic infected from both strains	0.1627	
γ_A	Recovery rate of asymptomatic infected from both strains	0.134	[20]
γ_D	Recovery rate of diagnosed isolated individuals	0.2	[20]
θ	Modification factor of asymptomatic infectiousness	0.0342	[20]
q_{r0}	Maximum quarantine fraction of resident lineage	vary	chosen
q_{m0}	Maximum quarantine fraction of mutant strain	vary	chosen
$\frac{1}{\omega}$	Maximum capacity of testing per day	vary	
δ_{rI}	Fastest diagnose rate of symptomatic infected resident lineage	0.333	chosen
δ_{mI}	Fastest diagnose rate of symptomatic infected mutant strain	0.333	chosen
δ_{rq}	Fastest diagnose rate of exposed individuals resident lineage	0.1237	[20]
δ_{mq}	Fastest diagnose rate of exposed to mutant strain	0.1237	[20]
p	Fraction of diagnosed cases further tested for WGS test	vary	chosen

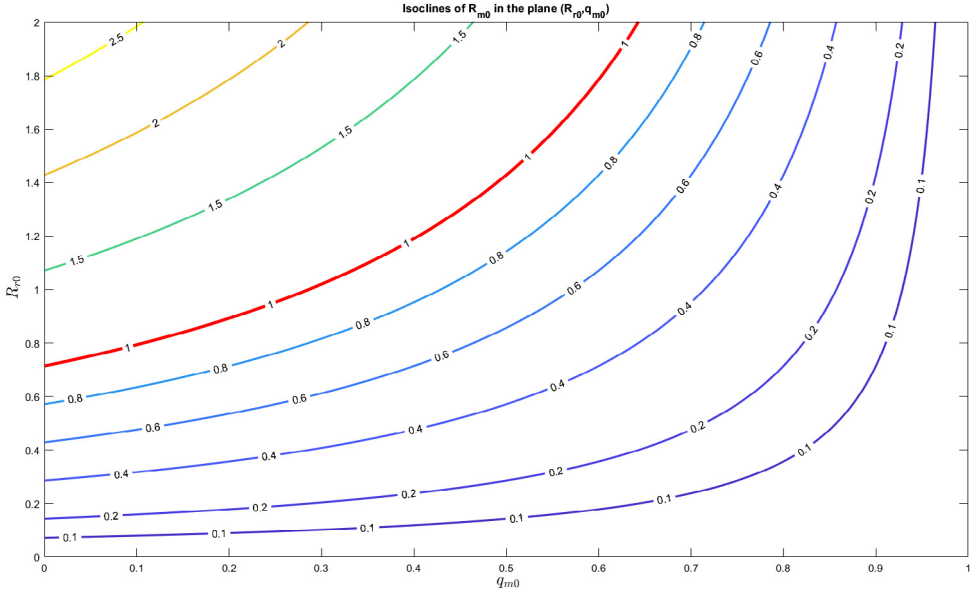

Fig. 3. Isoclines of effective reproduction number R_{m0} of m-vstrain/VOC, in plane (R_{r0}, q_{m0}), where red line represents $R_{m0} = 1$.

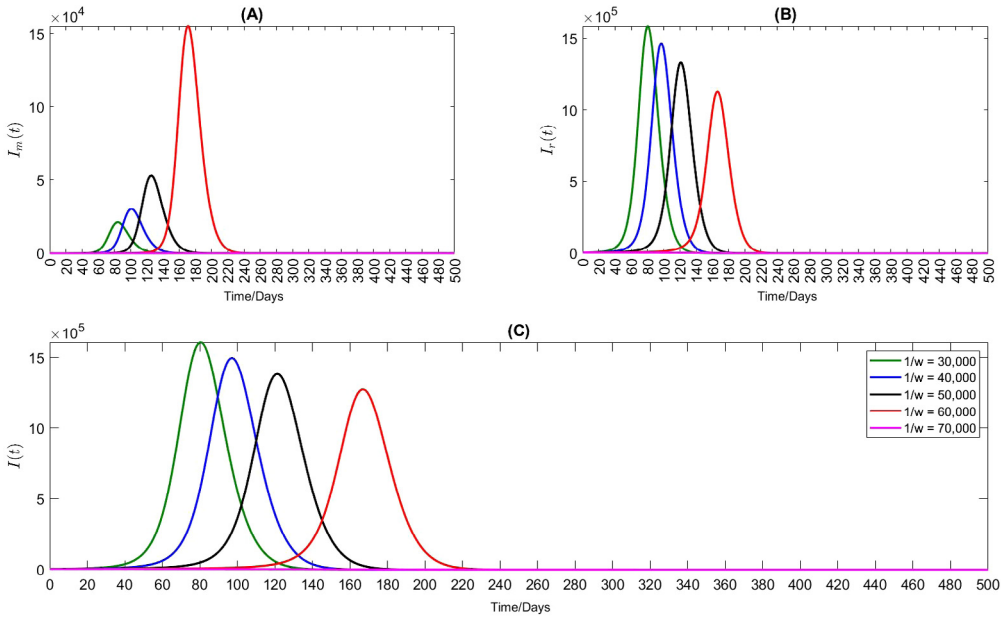

Fig. 4. The impact of varying the maximum capacity on disease prevalence with delays $(\tau_1, \tau_2) = (1, 3)$ and quarantine fraction $(q_{r0}, q_{m0}) = (0.4, 0.4)$. Plots (A) and (B) represent number of infections with m-strain ($I_m(t)$) and r-lineage ($I_r(t)$) respectively, plot (C) shows total number of infections $I(t) = I_m(t) + I_r(t)$.

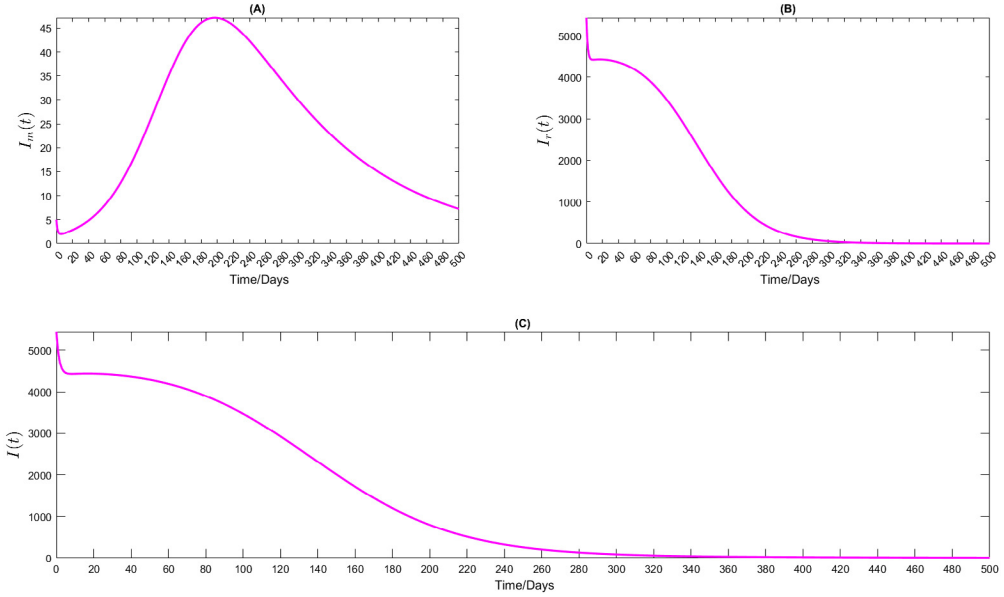

Fig. 5. This plot shows with high resolution the case in Fig. 4 with the maximum capacity 70,000. Note that the scale of the infections in this plot is several orders of magnitude smaller than Fig. 4.

2.4.2. *Impact of testing capacity and delays*

We now examine the impact of testing capacity w and test-tracing-quarantine delays τ_1 and τ_2 on disease prevalence when COVID-19 clinically confirmed cases are receiving further WGS testing.

For the simulations reported below, we vary the maximum testing capacity per day from 30,000 to 70,000 and take different combinations of both delays (1, 3), (1, 4), (2, 3) and (2, 4). We consider an ideal situation in which resources allow for a maximum of 80% successful contact tracing, with baseline scenario where $q_{r0} = 40\%$, $q_{m0} = 40\%$. We assume that the initial cases with VOC are $I_{m0} = 5$, which are relatively small compared with the cases I_{r0} of predominant resident lineage. We run our simulations for a period of 500 days.

Fig. 4 highlights the impact of varying the maximum testing capacity per day when delays are $(\tau_1, \tau_2) = (1, 3)$. We observe that by increasing the testing capacity from 30,000 to 60,000, the peak time for the r-lineage outbreak (plot (B)) is postponed and peak value is reduced. The peak time for the m-strain is also postponed, however, against the intuition, the peak number of infections with m-strain increases (plot (A)). This is because the r-lineage is dominant at the beginning of the outbreak, with much higher number of initial infections as compared to the m-strain; so if more testing is done per day more cases of r-lineage are diagnosed and isolated. As a result, it speeds up the frequency of the m-strain and speeds up the transmission of m-strain. However, for the total number of infections (with either r-lineage and m-strain), the large the testing capacity, the later the outbreak peak and the smaller the peak value (plot (C)). The peak time is delayed by 100 days and the number of infections at the peak time is reduced by more than 20% from 30,000 to 60,000 of testing capacity. Fig. 5 shows the significance of large testing capacity. It shows that the outcome with the testing capacity increased 70%, with $(\tau_1, \tau_2) = (1, 3)$. In this case,

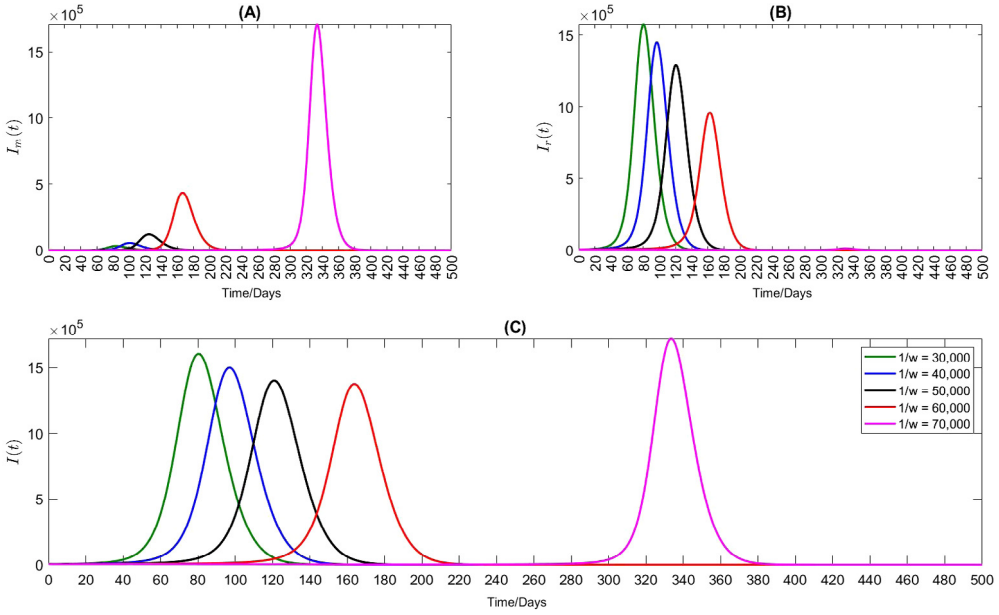

Fig. 6. The impact of varying the maximum capacity on disease prevalence with delays $(\tau_1, \tau_2) = (1, 4)$ and quarantine fractions $(q_{r0}, q_{m0}) = (0.4, 0.4)$, Plots (A) and (B) represent the numbers of infections with m-strain ($I_m(t)$) and r-lineage ($I_r(t)$) respectively, plot (C) shows the number of total infections $I(t) = I_m(t) + I_r(t)$.

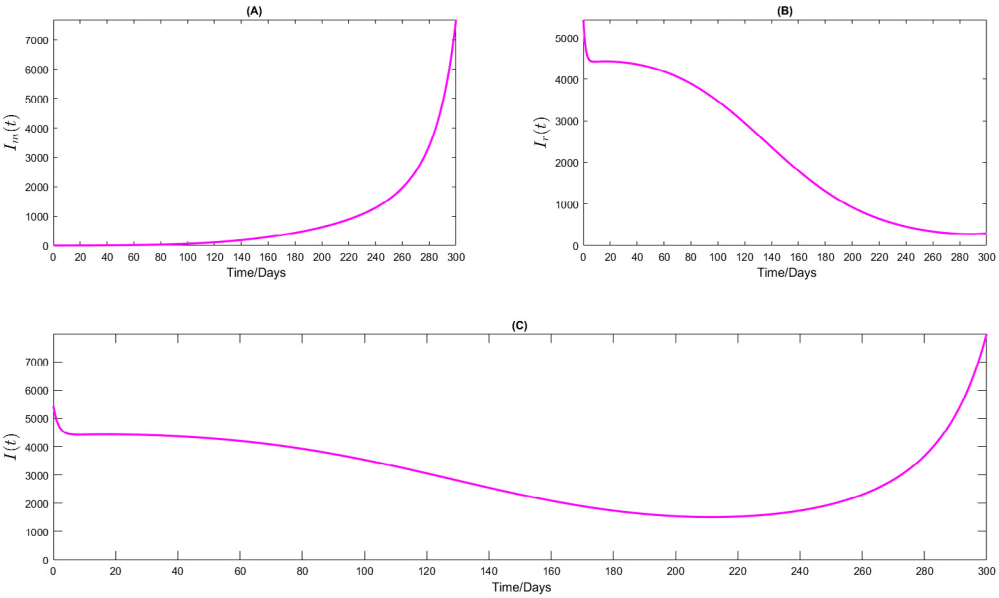

Fig. 7. This plot shows with high resolution the case in Fig. 6 with the maximum capacity 70,000, where the time scale analyzed extends for 300 days. Note that the scale of the infections in this plot is several orders of magnitude smaller than Fig. 6.

an outbreak by r-lineage is completely prevented (Plot (B)); while an outbreak by m-strain is not prevented, its outbreak is very small with the only 45 cases at the peak time (Plot (A)). Adding them together, we notice an overall declining trend for the total cases.

Fig. 6 illustrates the effect of testing capacities on prevalence, by increasing one more day in the WGS test delay $(\tau_1, \tau_2) = (1, 4)$. In this case, for the capacity from 30,000 to 60,000, the epidemic results are similar to that with delay (1, 3) (Fig. 4).

However, with 70,000 testing capacity, the results are dramatically different for mutant strain and the total number of infections. Under this delay structure, infections with m-strain continue to increase slowly and dominate the r-lineage. Fig. 7 clearly displays this aspect. We can see in plot (A), infections with m-strain rise and in plot (B), infection with r-lineage declines slowly. It can be noted that overall prevalence (plot (C)) first decreases and then starts to rise quickly after about 210 days, leading to an outbreak. Which shows that in this specific case, m-strain has established and dominates the r-lineage.

Delay in the WGS testing triggers delay in the strain-specific interventions, specially the tracing and quarantine. We show what happens when τ_2 is increased from 3 days to 4-days in Fig. 6 plot (A): not only the peak values of infections increase compared with the situation of $(\tau_1, \tau_2) = (1, 3)$, (Fig. 4 plot (A)) with the same testing capacity, but more importantly, when the maximum capacity is 70,000 per day, increasing the value of τ_2 by one day significantly changes the outcome from outbreak being avoided to a large m-strain induced outbreak. After the clinical COVID-19 testing, a fraction of contacts is traced and quarantined, but the others (exposed to the m-strain) escaped from the tracing when WGS testing is delayed and contribute to the spread in the population.

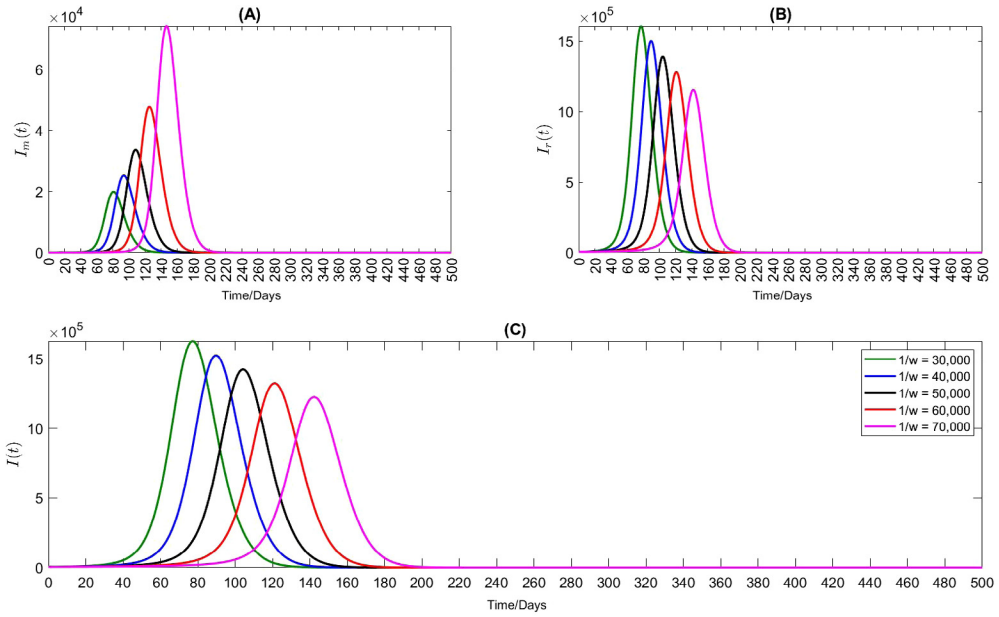

Fig. 8. The impact of increasing the maximum capacity on disease prevalence with delays $(\tau_1, \tau_2) = (2, 3)$. Plot (A) represents the case where infections with m-strain ($I_m(t)$ are rising and (B) shows the declining trend in the number of infections with r-lineage when we increase the maximum capacity. Plot (C) shows the total number of infections $I(t) = I_m(t) + I_r(t)$ with decreasing trend and peak time delayed.

To consider the impact of delaying the clinical COVID-19 test for case identification, we consider the situation where $(\tau_1, \tau_2) = (2, 3)$ subject to different levels of testing capacities, and we report the simulations in Fig. 8. In comparison to Fig. 4, we notice that with an additional day of delay in clinical testing would lead to a surge in infections even with the testing capacity of 70,000 per day. In addition, the peak time is advanced significantly. For example, with testing capacity of 60,000, the peak time changes from 180 days to 120 days with τ_1 increasing from 1 to 2 days. Therefore, a single day delay in testing can result in peak time shorten by several weeks.

In summary, we conclude that the final outcome in terms of both r-lineage and m-strain after an introduction of the m-strain depends not only on the maximum testing capacity but also on both clinical and WGS testing delays and their combination. For example, in the scenarios discussed above, the testing delays (1, 3) coupled with a testing capacity of 70,000 per day avoid a new outbreak despite the initial increase of m-strain infections.

2.4.3. Targeted tracing and quarantine efforts

We now consider the issue of optimizing public health resources with designated efforts of increasing the WGS testing and enhancing the tracing and quarantine effort for contacts of the confirmed m-strain cases.

We assume that public health system is able to trace and isolate 40%–70% of cases after the clinical COVID-19 test, and we aim to find the minimal amount of additional efforts needed in tracing contacts of m-strain cases after their strains have been confirmed through the WGS testing in order to avoid or mitigate a VOC-induced outbreak.

We have produced extensive simulations for different combinations of testing capacity, testing delays (1, 3), (2, 3), (1, 4) and (2, 4), when the maximum quarantine fractions are in the range $q_{r0} = 40\%$–70% and $q_{m0} = 0\%$–30% to see whether it may or may not prevent an outbreak. First, we have found that if the testing capacity is low (30,000–40,000), we need very strong contact tracing in COVID-19 clinical testing ($q_{r0} = 70\%$), and very stringent additional tracing and quarantine of m-strain cases contacts after their WGS confirmation are required. So, in what follows, we focus on the case where COVID-19 test capacity is between 50,000–70,000. We summarize our simulations in Tables 3–5.

With 50,000 testing capacity, as shown in Table 3, an outbreak cannot be prevented under any realistic combinations of testing delays, when we consider the parameters in the following range $q_{r0} = 40\%$–50% and $q_{m0} = 0\%$–30%. Increasing q_{r0} to 60%, as shown in Fig. 9, subplots (A) and (B), the outbreak can be prevented if the testing delay is one day. (noting the scale of the cases for two different strains). The simulations also show that given such a short and unrealistic testing delay, additional strain-specific tracing would not make much difference. We also note that if the testing delay of COVID-19 is longer than one day, i.e. $(\tau_1, \tau_2) = (2, 3)$, Fig. 9, subplots (C) and (D), an outbreak will occur involving both the resident lineage and the m-strain . In this case, even an intensive strain-specific tracing and quarantine $q_{m0} = 30\%$ cannot control the epidemic. Finally, $q_{r0} = 70\%$ yields similar results to the case of $q_{r0} = 60\%$ with clinical COVID test delay as one day. However, Fig. 10 which includes a two days delay (2, 3) in clinical COVID testing shows that epidemic can still be controlled if the VOC-specific quarantine fraction is in the range 10%–30%. In addition, when $q_{m0} = 10\%$–30%, VOC cases rise and a small outbreak occurs while resident lineage cases decrease monotonically. If we exclude VOC-specific quarantine, VOC-strain infections rise, resident lineage infections do not monotonically decrease but instead the number of cases starts growing rapidly and then fall a few days later. If we compare Fig. 10 with Fig. 9, subplots (C) and (D), we can see that with same delays and testing capacity, outbreaks can be controlled not only by increasing q_{r0} but also by q_{m0}.

We then consider the case with testing capacity of 60,000 and by varying the delays of tests. The results are summarized in Table 4.

Similarly to the previous case, there is an outbreak of disease for a 40% quarantine fraction after clinical testing, whatever the choices of q_{m0} and delays. However, in the case when quarantine fractions are $(q_{r0}, q_{m0}) = (50\%, 0\%$–$30\%)$ and delays (1, 3) or (1,4), we found that there is a declining trend with resident lineage in time and VOC cases rise very slowly without VOC-specific quarantine (i.e. $(q_{m0} = 0)$, and a very small VOC-outbreak with $q_{m0} = 10\%$–30%. So, overall the disease stays under control. We note that with the same testing delays (1, 3) and a 10% increase in the quarantine fraction $q_{r0} = 60\%$, the transmission dynamics is that same as with testing capacity 50,000, and total infection declines and dies out. Similar results are observed with delays (1, 4). However, with an additional testing delay (i.e., (2,3), (2, 4)) and with $q_{r0} = 50\%$, the disease cannot be controlled and there would be an outbreak even we have a high level of additional VOC-specific quarantine (0%–30%). Though, with $q_{r0} = 60\%$, as shown in

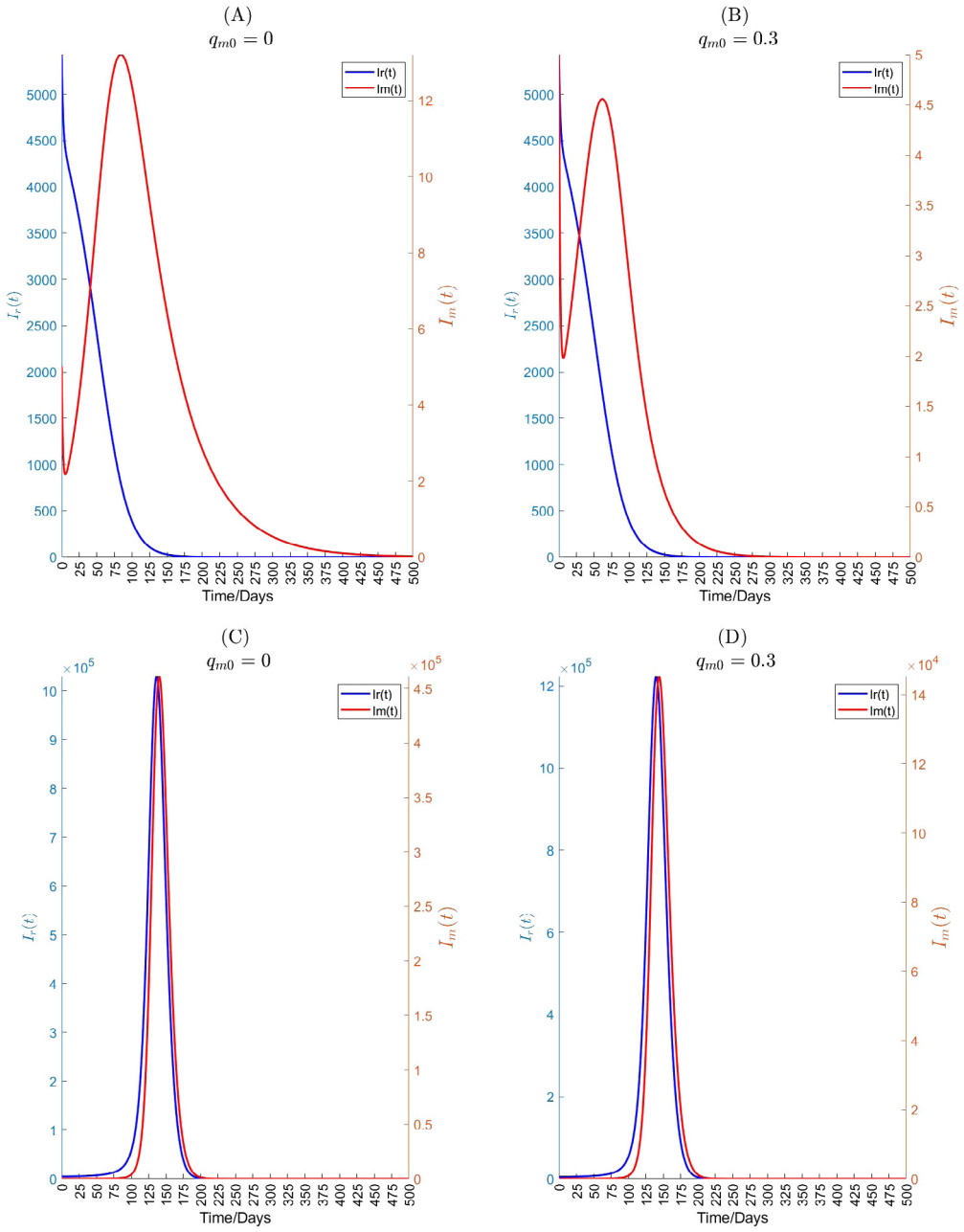

Fig. 9. The impact of intensive VOC-specific quarantine ($q_{m0} = 0\%, 30\%$) after WGS test on the number of infections $I_m(t)$ with m-strain (red with scale on right side) and $I_r(t)$ with resident lineage (blue with scale on left side). We hold quarantine fraction ($q_{r0} = 0.6$) after clinical COVID-19 test with testing capacity 50,000 per day and testing delays $(\tau_1, \tau_2) = (1, 3)$ in subplots (A), (B) and $(\tau_1, \tau_2) = (2, 3)$ in subplots (C), (D). Note that the scales for r-lineage and for the m-strain are different. With delay (1,3) subplots (A and B) at the peak of a tiny outbreak by m-strain, we have only 6 cases and the r-lineage is under control. While with one day more testing delay $(\tau_1, \tau_2) = (2, 3)$ (subplots C and D) there is an outbreak with both r-lineage and m-strain.

Fig. 11, infections with r-linage decline and infections with m-strain are significantly slowed down with a small outbreak (total number of infections under control) with 20% or more VOC-specific quarantine fraction.

But with only 10% VOC-specific quarantine, resident lineage infections go down first but then start to rise, leading to an outbreak of both r-lineage and m-strain. Therefore, increasing VOC-specific quarantine may help to control not only VOC infections but also r-lineage infections.

On the other hand, as shown in Fig. 12 a longer delay in WGS testing (2, 4) leads to an outbreak that cannot be prevented even ($q_{m0} = 30\%$). Recall that if ($q_{r0} = 70\%$), the disease is under control with any combination of delays regardless of VOC-specific quarantine.

Finally, we increase the testing capacity to 70,000, and the results are shown in Table 5. In this scenario, most of the results are similar to the 60,000 testing capacity case with $q_{r0} = 40\%$–50% and any test delays. Also, with testing delays (1, 3) and $q_{r0} = 60\%$, the epidemics stays under control without requiring any VOC-specific quarantine. But an additional day delay in clinical COVID-19 testing (2, 3) (see Fig. 13) leads to a m-strain outbreak and so we see an overall prevalence increases without additional VOC-specific quarantine. However, a small increase of VOC-specific quarantine by 10% eases the situation, the m-strain infections rise slowly, slowing down the replacement. On the other hand, with an intensive VOC-specific quarantine 20% or 30%, cases with mutant strain initially rise up but then eventually decrease. Finally, we notice that an additional one day delay in WGS test (2,

Table 3
Table summarizes the simulation results for the overall infections (total infections) with m-strain and r-lineage. We consider a fixed maximum 50,000 testing capacity per day and study different combinations of delays (1,3), (2,3), (1,4), (2,4) for COVID-19 clinical tests and WGS testing, and quarantine fractions (q_{r0}, q_{m0}).

Maximum testing capacity 50,000				
Delay/ (q_{r0}, q_{m0})	(1, 3)	(2, 3)	(1, 4)	(2, 4)
(0.4,0)				
(0.4,0.1)	Outbreak			
(0.4,0.2)				
(0.4,0.3)				
(0.5,0)				
(0.5,0.1)	Outbreak			
(0.5,0.2)				
(0.5,0.3)				
(0.6,0)				
(0.6,0.1)	Under control	Outbreak	Under control	Outbreak
(0.6,0.2)				
(0.6,0.3)				
(0.7,0)		Outbreak		Outbreak with VOC
(0.7,0.1)	Under control	Small outbreak with VOC, Overall controlled	Under control	
(0.7,0.2)				Small outbreak with VOC, Overall controlled
(0.7,0.3)				

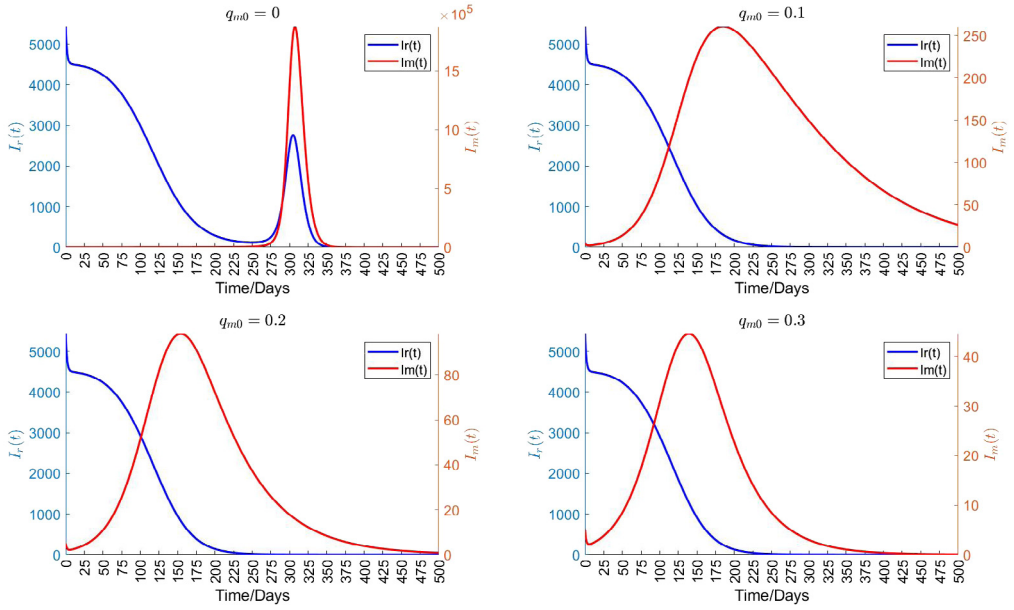

Fig. 10. The impact of VOC-specific quarantine (q_{m0}) on the number of infections with m-strain and resident lineage. Quarantine fraction $(q_{r0} = 0.7)$ after clinical COVID-19 test and testing capacity (50,000 per day). The testing delays are $(\tau_1, \tau_2) = (2, 3)$.

4) would produce a VOC outbreak with or without any VOC-specific quarantine measure.

In summary, we infer from our comparative simulations that if the maximum testing capacity maintains to at 60,000–70,000 with minimal delay of one day (delays are then (1,3) and (1,4)) in COVID-19 test, then (i) with 50% quarantine the disease can be slowed down or prevented by increasing VOC-specific quarantine; (ii) $q_{r0} = 60\%$ can control both strains without any additional VOC-specific quarantine. As delay increases to one more day (2,3) and (2,4) more VOC-specific quarantine would be required to control epidemic.

We also simulated a scenario in which not every positive case receives the WGS testing. Namely, considering different WGS testing capacity, we notice that if less confirmed cases receive the WGS test, VOC-infections and the total infections rise and the peak may arrive earlier. This will create sharp and rapid increase for hospitalization and ICU beds. We presented an illustration in Fig. 14, where only 5% COVID-19 positive tests receive further WGS test. Comparing Fig. 14 with Fig. 4 (when every COVID positive case is going through additional WSG test), we observe in the case of 70,000 testing capacity, peak of infections (with only 5% WGS test) can arrive 100 days earlier.

3. Discussion and conclusion

We developed a two strain transmission dynamics model to understand the situation when an existing r-lineage is under control with some social distancing measures including quarantine, but a more transmissible m-strain (VOC) is introduced. We considered the situation where (1) the COVID-19 testing capacity is limited and WGS testing capacity to determine the strain is even more so; (2) each test and each tracing and quarantine of the contacts of confirmed cases takes a certain amount of time, so the more infections to be tested the longer delay for testing triggered contact tracing and quarantine. We

Table 4
Table summarizes the simulation results of overall infections (total infections) with m-strain and r-lineage. We consider a fixed maximum 60,000 testing capacity per day and study different combinations of delays (1,3), (2,3), (1,4), (2,4) for COVID-19 clinical tests and WGS testing, and quarantine fractions (q_{r0}, q_{m0}).

Maximum testing capacity 60,000				
Delay/ (q_{r0}, q_{m0})	(1,3)	(2,3)	(1,4)	(2,4)
(0.4,0)	Outbreak			
(0.4,0.1)				
(0.4,0.2)				
(0.4,0.3)				
(0.5,0)	Slow outbreak with VOC		Slow outbreak with VOC	
(0.5,0.1)	Small outbreak with VOC, Overall controlled	Outbreak	Small outbreak with VOC, Overall controlled	Outbreak
(0.5,0.2)				
(0.5,0.3)				
(0.6,0)	Under control	Outbreak	Under control	Outbreak
(0.6,0.1)				
(0.6,0.2)		Small outbreak with VOC, Overall controlled		
(0.6,0.3)				
(0.7,0)	Under control	Very small outbreak with VOC, Overall controlled	Under control	Very small outbreak with VOC, Overall controlled
(0.7,0.1)				
(0.7,0.2)				
(0.7,0.3)				

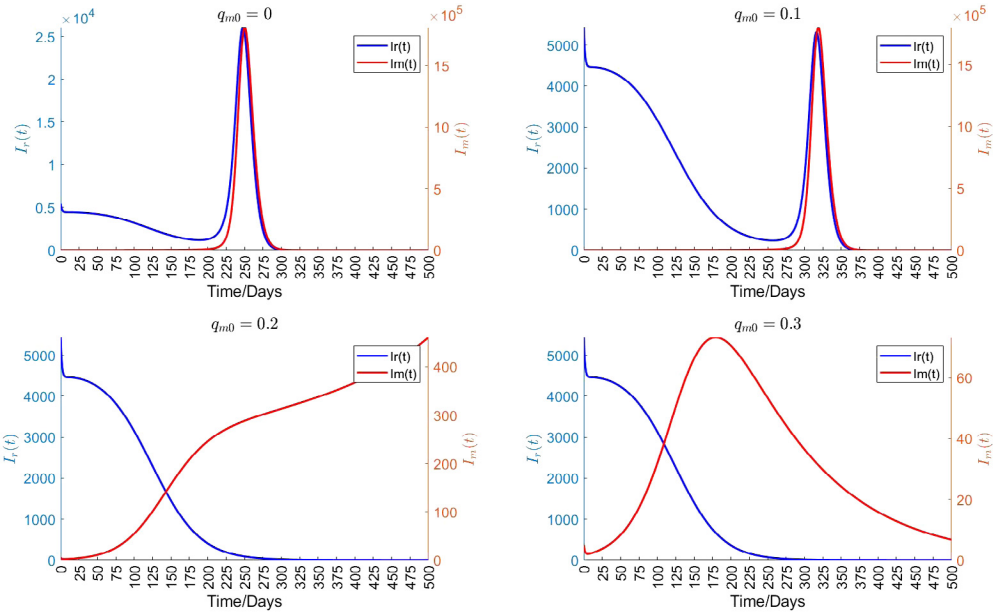

Fig. 11. The impact of VOC-specific quarantine $(q_{m0} = 0\%, 10\%, 20\%30\%)$ on number of infections with m-strain and resident lineage. Quarantine fraction is $(q_{r0} = 0.6)$ and testing capacity is 60,000 and the testing delays are $(\tau_1, \tau_2) = (2, 3)$.

use the Holling type saturation function to describe these limitations, and we aim to assess the role of tracing delay and variant-specific intensified quarantine in preventing the replacement and outbreak of an VOC-induced outbreak.

We first showed that the control reproduction number of VOC $R_{m0} < 1$, if the control reproduction number of r-lineage $R_{r0} \leq \frac{1}{\kappa}$ with $\kappa > 1$ being the relative transmissibility of the m-strain over the r-lineage. If this is not possible, a large amount of VOC cases may require to be tracked after WGS test. Our simulation results show that the epidemic growth with VOC depends not only on testing capacity but also on testing delays. In particular, increasing significantly the maximum testing capacity for COVID-19 confirmation and WGS tests can defer the outbreak peak time as well as decrease the peak value, however, lukewarm tracing and quarantine can potentially increase the VOC-cases at the outbreak peak time. We exploited further how regular Covid-19 testing (PCR, antibody and/or antigen) delay increases the chance of an outbreak and the outbreak severity in terms of the total and VOC-cases at the peak time. In addition, we showed that if delay in WGS test cannot be reduced from four days, in the case study of the Province of Ontario, Canada, then the reduction of COVID-19 clinical test delay to one day and strain-specific quarantine combined is needed and can play a significant role in mitigating the epidemic. Our results supported the fact that a certain level of daily test capacity, 60,000 test per day in the Province of Ontario, must be maintained in order for the testing-to quarantine intervention to be effective. We calculated that with this minimal testing capacity, a quarantine proportion of no less than 40% is needed if we want the strain-specific quarantine after WGS be useful to prevent an VOC-induced outbreak. We also illustrated that the normal quarantine proportion should be increased to 50% then only less intensive strain-specific quarantine is required.

In conclusion, our analyses suggest that a combination of large COVID-19 clinical test capacity, a short delay in both the clinical test

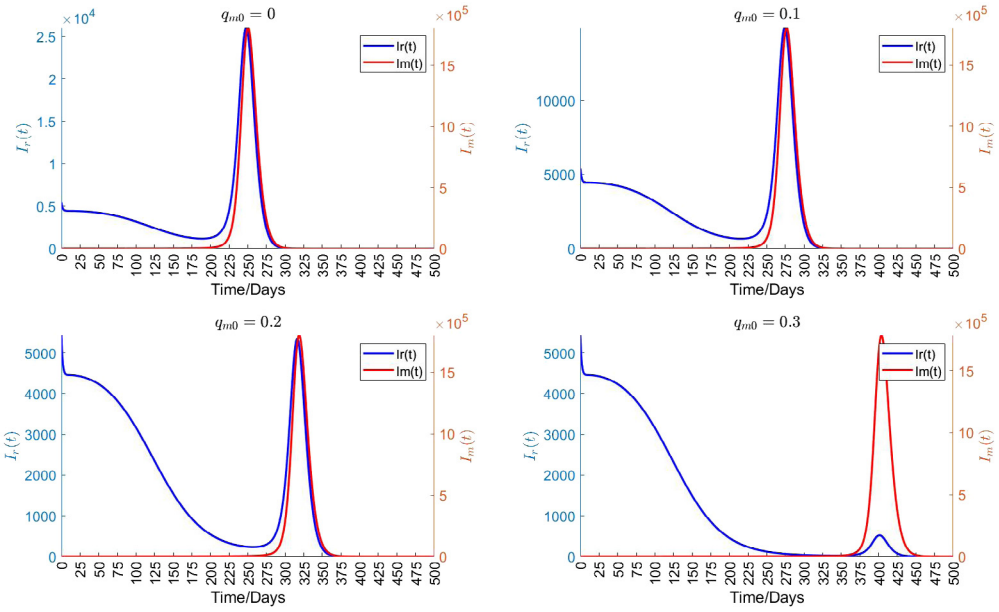

Fig. 12. The impact of VOC-specific quarantine (q_{m0}) on the numbers of infections with m-strain and resident linage. Quarantine fraction q_{r0} after clinical COVID-19 test and testing capacity are the same as in Fig. 11. The testing delays are different: $(\tau_1, \tau_2) = (2, 4)$.

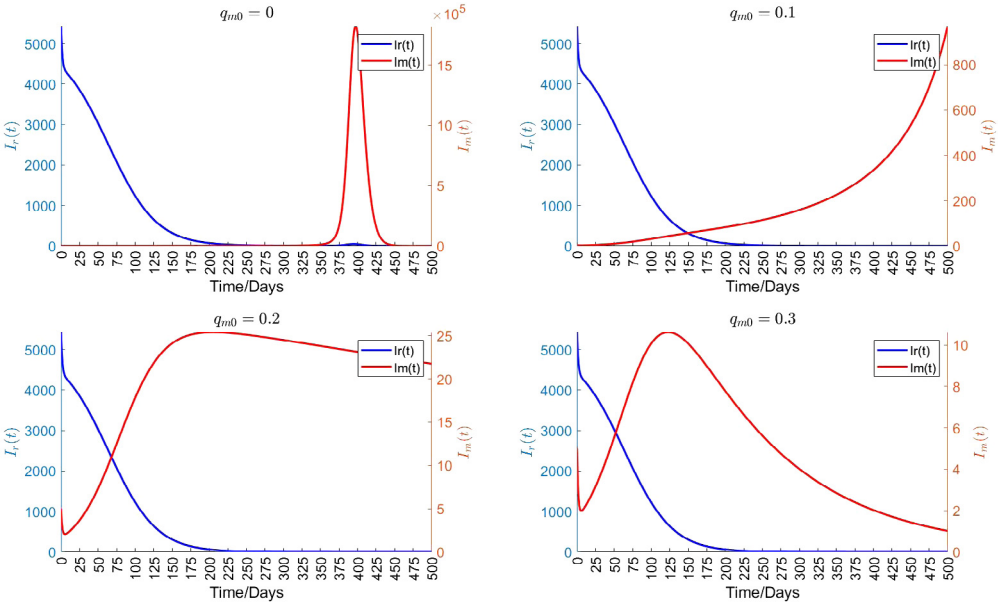

Fig. 13. The impact of VOC-specific quarantine (q_{m0}) on the number of infections with m-strain and resident lineage. Quarantine fraction is ($q_{r0} = 0.6$) and testing capacity is 70,000 per day. The testing delays are $(\tau_1, \tau_2) = (2, 3)$.

and WGS test and the subsequent contact-tracing and quarantine, and moderate level of additional strain-specific quarantine is a feasible and optimal approach to prevent or mitigate a VOC-driven outbreak. Given this conclusion, we suggest that budgetary consideration for testing should not prevent WGS testing from occurring at the expense of first and concomitant quarantine of traced contacts that were not infected. Given the value of WGS and the additional strain-specific interventions, our study calls for investment of WGS testing capacity.

Declaration of competing interest

The authors declare that they have no known competing financial interests or personal relationships that could have appeared to influence the work reported in this paper.

Acknowledgments

This project has been partially supported by the Canadian Institute of Health Research (CIHR) 2019 Novel Coronavirus (COVID-19) rapid research program. JW is a member of the Ontario COVID-19 Modelling Consensus Table, and a member of the Expert Panel of the Public Health Agency of Canada (PHAC) Modeling group. This research was presented to both the Ontario Table and PHAC group. Reported COVID-19 cases were obtained from the Public Health Ontario (PHO) integrated Public Health Information System (iPHIS), via the Ontario COVID-19 Modelling Consensus Table.

Table 5
Table representing the simulation results of overall infections (total infections) with m-strain and r-lineage. We consider a fixed maximum 70,000 testing capacity per day and study different combinations of delay structures (1,3), (2,3), (1,4), (2,4) for COVID-19 clinical tests and WGS testing for VOC and quarantine fractions (q_{r0}, q_{m0}).

Maximum testing capacity 70,000				
Delay/ (q_{r0}, q_{m0})	(1,3)	(2,3)	(1,4)	(2,4)
(0.4,0) (0.4,0.1) (0.4,0.2) (0.4,0.3)	Outbreak			
(0.5,0) (0.5,0.1) (0.5,0.2) (0.5,0.3)	Slow outbreak with VOC very small outbreak with VOC, Overall under control	Outbreak	Slow outbreak with VOC very small outbreak with VOC, Overall under control	Outbreak
(0.6,0) (0.6,0.1) (0.6,0.2) (0.6,0.3)	Under control	Outbreak with VOC Slow outbreak with VOC Small outbreak with VOC, Overall controlled	Under control	r-lineage under control, Outbreak with VOC
(0.7,0) (0.7,0.1) (0.7,0.2) (0.7,0.3)	Under control	Underll control	Under control	Very small outbreak with VOC, Overall controlled

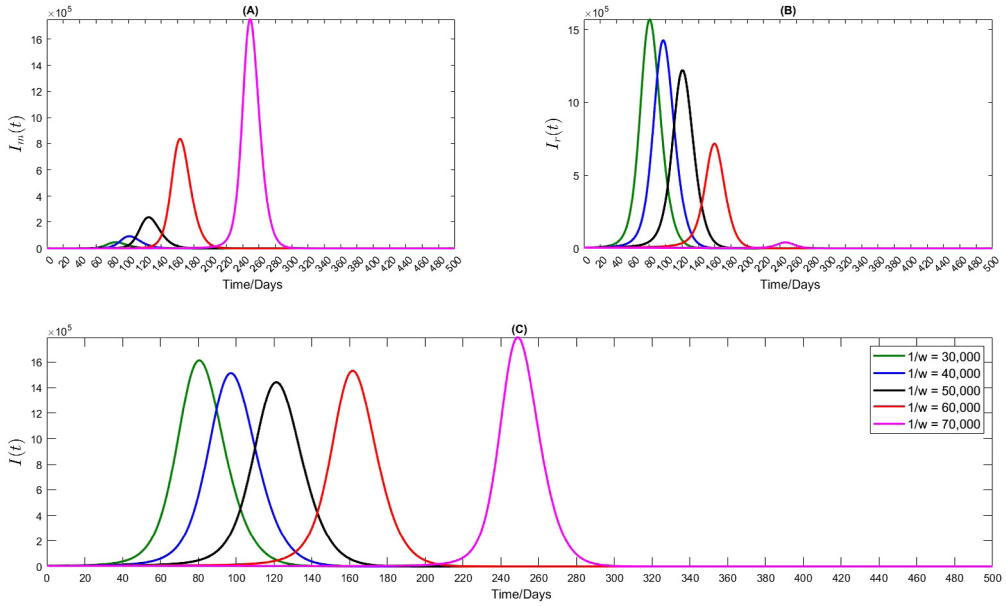

Fig. 14. The impact of WGS testing capacity on disease prevalence with testing delays $(\tau_1, \tau_2) = (1, 4)$, when only 5% of confirmed cases receive further WGS testing. Plots (A) and (B) give the numbers of infections with m-strain $(I_m(t))$ and r-lineage $(I_r(t))$ respectively, plot (C) shows the total number of infections $I(t) = I_m(t) + I_r(t)$.

References

[1] M. Pachetti, B. Marini, F. Benedetti, F. Giudici, E. Mauro, P. Storici, C. Masciovecchio, S. Angeletti, M. Ciccozzi, R.C. Gallo, et al., Emerging SARS-CoV-2 mutation hot spots include a novel RNA-dependent-RNA polymerase variant, J. Transl. Med. 18 (1) (2020) 1–9, http://dx.doi.org/10.1186/s12967-020-02344-6.

[2] J.E. Lemieux, J.Z. Li, Uncovering ways that emerging severe acute respiratory syndrome coronavirus 2 lineages may increase transmissibility, J. Infect. Dis. (2021) http://dx.doi.org/10.1093/infdis/jiab083.

[3] B. Korber, W.M. Fischer, S. Gnanakaran, H. Yoon, J. Theiler, W. Abfalterer, N. Hengartner, E.E. Giorgi, T. Bhattacharya, B. Foley, et al., Tracking changes in SARS-CoV-2 spike: evidence that D614G increases infectivity of the COVID-19 virus, Cell 182 (4) (2020) 812–827, http://dx.doi.org/10.1016/j.cell.2020.06.043.

[4] P. England, SARS-CoV-2 Variants of Concern and Variants under Investigation in England, vol. 11, Public Health England, 2021.

[5] T. Kirby, New variant of SARS-CoV-2 in UK causes surge of COVID-19, Lancet Respir. Med. 9 (2) (2021) e20–e21, http://dx.doi.org/10.1016/S2213-2600(21)00005-9.

[6] S. Celaschi, The impact of SARS-CoV-2 variant to COVID-19 epidemic in Brazil, 2020, medRxiv, http://dx.doi.org/10.1101/2020.09.25.20201558.

[7] H. Tegally, E. Wilkinson, R.J. Lessells, J. Giandhari, S. Pillay, N. Msomi, K. Mlisana, J. Bhiman, M. Allam, A. Ismail, et al., Major new lineages of SARS-CoV-2 emerge and spread in South Africa during lockdown, 2020, medRxiv, http://dx.doi.org/10.1101/2020.10.28.20221143.

[8] Updates on COVID-19 Variants of concern, URL https://nccid.ca/covid-19-variants/.

[9] Genomic Surveillance for SARS-CoV-2 Variants, URL https://www.cdc.gov/coronavirus/2019-ncov/cases-updates/variant-surveillance.html.

[10] A.J. Kucharski, P. Klepac, A.J. Conlan, S.M. Kissler, M.L. Tang, H. Fry, J.R. Gog, W.J. Edmunds, J.C. Emery, G. Medley, et al., Effectiveness of isolation, testing, contact tracing and physical distancing on reducing transmission of SARS-CoV-2 in different settings: a mathematical modelling study, Lancet Infect. Dis. 20 (10) (2020) 1151–1160, http://dx.doi.org/10.1016/S1473-3099(20)30457-6.

[11] B. Tang, F. Xia, S. Tang, N.L. Bragazzi, Q. Li, X. Sun, J. Liang, Y. Xiao, J. Wu, The effectiveness of quarantine and isolation determine the trend of the COVID-19 epidemics in the final phase of the current outbreak in China, Int. J. Infect. Dis. 95 (2020) 288–293, http://dx.doi.org/10.1016/j.ijid.2020.03.018.

[12] C.N. Ngonghala, E. Iboi, S. Eikenberry, M. Scotch, C.R. MacIntyre, M.H. Bonds, A.B. Gumel, Mathematical assessment of the impact of non-pharmaceutical interventions on curtailing the 2019 novel coronavirus, Math. Biosci. 325 (2020) 108364, http://dx.doi.org/10.1016/j.mbs.2020.108364.

[13] M.E. Kretzschmar, G. Rozhnova, M.C. Bootsma, M. van Boven, J.H. van de Wijgert, M.J. Bonten, Impact of delays on effectiveness of contact tracing

strategies for COVID-19: a modelling study, Lancet Public Health 5 (8) (2020) e452–e459, http://dx.doi.org/10.1016/S2468-2667(20)30157-2.

[14] J. Hellewell, S. Abbott, A. Gimma, N.I. Bosse, C.I. Jarvis, T.W. Russell, J.D. Munday, A.J. Kucharski, W.J. Edmunds, F. Sun, et al., Feasibility of controlling COVID-19 outbreaks by isolation of cases and contacts, Lancet Glob. Health 8 (4) (2020) e488–e496, http://dx.doi.org/10.1016/S2214-109X(20)30074-7.

[15] L. Ferretti, C. Wymant, M. Kendall, L. Zhao, A. Nurtay, L. Abeler-Dörner, M. Parker, D. Bonsall, C. Fraser, Quantifying SARS-CoV-2 transmission suggests epidemic control with digital contact tracing, Science 368 (6491) (2020) http://dx.doi.org/10.1126/science.abb6936.

[16] N.G. Davies, S. Abbott, R.C. Barnard, C.I. Jarvis, A.J. Kucharski, J.D. Munday, C.A. Pearson, T.W. Russell, D.C. Tully, A.D. Washburne, et al., Estimated transmissibility and impact of SARS-CoV-2 lineage B. 1.1. 7 in England, Science 372 (6538) (2021) http://dx.doi.org/10.1126/science.abg3055.

[17] E. Volz, S. Mishra, M. Chand, J.C. Barrett, R. Johnson, L. Geidelberg, W.R. Hinsley, D.J. Laydon, G. Dabrera, A. O'Toole, et al., Transmission of SARS-CoV-2 lineage B. 1.1. 7 in England: Insights from linking epidemiological and genetic data, 2021, MedRxiv, 2020–12, http://dx.doi.org/10.1101/2020.12.30.20249034.

[18] J. Wu, F. Scarabel, B. Majeed, N.L. Bragazzi, J. Orbinski, The impact of public health interventions on delaying and mitigating against replacement by SARS-CoV-2 variants of concern, 2021, Available at SSRN 3779007, http://dx.doi.org/10.2139/ssrn.3779007.

[19] G. Gonzalez-Parra, D. Martínez-Rodríguez, R.J. Villanueva-Micó, Impact of a new SARS-CoV-2 variant on the population: A mathematical modeling approach, Math. Comput. Appl. 26 (2) (2021) 25, http://dx.doi.org/10.3390/mca26020025.

[20] B. Tang, F. Scarabel, N.L. Bragazzi, Z. McCarthy, M. Glazer, Y. Xiao, J.M. Heffernan, A. Asgary, N.H. Ogden, J. Wu, De-escalation by reversing the escalation with a stronger synergistic package of contact tracing, quarantine, isolation and personal protection: feasibility of preventing a COVID-19 rebound in Ontario, Canada, as a case study, Biology 9 (5) (2020) 100, http://dx.doi.org/10.3390/jcm9020462.

[21] O. Diekmann, J.A.P. Heesterbeek, J.A. Metz, On the definition and the computation of the basic reproduction ratio R 0 in models for infectious diseases in heterogeneous populations, J. Math. Biol. 28 (4) (1990) 365–382, http://dx.doi.org/10.1007/BF00178324.

[22] J.M. Heffernan, R.J. Smith, L.M. Wahl, Perspectives on the basic reproductive ratio, J. R. Soc. Interface 2 (4) (2005) 281–293, http://dx.doi.org/10.1098/rsif.2005.0042.

[23] M. Li, X. Liang, Q. Jiang, et al., The latest understanding of the epidemiological characteristics of new coronavirus pneumonia, Chin. J. Epidemiol. 41, 139–143, http://dx.doi.org/10.3760/cma.j.issn.0254-6450.2020.02.002.

[24] B. Tang, X. Wang, Q. Li, N.L. Bragazzi, S. Tang, Y. Xiao, J. Wu, Estimation of the transmission risk of the 2019-nCoV and its implication for public health interventions, J. Clin. Med. 9 (2) (2020) 462, http://dx.doi.org/10.3390/jcm9020462.